# Finite Elements for Geometrical Minimal Shape

Vinicius F. Arcaro[1*], Katalin K. Klinka[2] and Dario A. Gasparini[3]

[1]*University of Campinas, College of Civil Engineering, Av. Albert Einstein 951, Campinas, SP 13083, Brazil*
[2]*Department of Structural Engineering, Budapest University of Technology and Economics, 2 Bertalan Lajos, Budapest, H-1111, Hungary*
[3]*Civil Engineering Department, Case Western Reserve University, 2182 Adelbert Rd., Cleveland, OH 44106, U.S.A.*
[*]*E-mail address: vinicius.arcaro@arcaro.org*

(Received November 2, 2012; Accepted August 23, 2013)

This text describes a novel mathematical model that unifies all geometrical minimal shape problems by defining geometrical finite elements. Three types of elements are defined: line, triangle and tetrahedron. By associating a volume for each element type, the elements can be used together in the discretization of a geometrical shape. For each element type, its corresponding isovolumetric element is also defined. The geometrical minimal shape problem is formulated as an equality constrained minimization problem. The importance of this approach is that apparently distinct problems can be treated by a unified framework. The augmented Lagrangian method is used to solve the associated unconstrained minimization problem. A quasi-Newton method is used, which avoids the evaluation of the Hessian matrix. The source and executable computer codes of the algorithm are available for download from the website of one of the authors.

**Key words:** Element, Finite, Form, Minimization, Nonlinear

## 1. Introduction

This text describes a mathematical model that unifies all geometrical minimal shape problems by defining geometrical finite elements. Three types of elements are defined: line, triangle and tetrahedron. The elements can be used together through the unifying concept of volume. For each element type, its corresponding isovolumetric element is also defined. The shape is discretized into line, triangle and tetrahedron elements. The elements are interconnected at their nodal points. The geometrical minimal shape problem is formulated as an equality constrained minimization problem. The augmented Lagrangian method is used to solve the associated unconstrained minimization problem. A quasi-Newton method is used, which avoids the evaluation of the Hessian matrix.

The following conventions apply unless otherwise specified or made clear by the context. A Greek letter expresses a scalar. A lower case letter represents a column vector.

## 2. Line Element Definition

Figure 1 shows the geometry of the line element for a 3D space. The nodes are labeled 1 and 2. The nodal displacements transform the element from its initial state to its final state.

$$\bar{v} = v + u^2 - u^1 \tag{1}$$

$$\|\bar{v}\| = (\bar{v}^T \bar{v})^{1/2}. \tag{2}$$

The previous expression can be written as:

$$\|\bar{v}\| = \left[v^T v + 2v^T(u^2 - u^1) + (u^2 - u^1)^T(u^2 - u^1)\right]^{1/2}. \tag{3}$$



### 2.1 Element final volume

Supposing that the line element has a fixed cross sectional area $\alpha$, its final volume can be written as:

$$\phi_e(u) = \alpha\|\bar{v}\|. \tag{4}$$

### 2.2 Gradient of the element final volume

The nodal displacements vectors are numbered according to its node numbers. Their individual components are numbered as follows:

$$u^1 = \begin{bmatrix} u_1 \\ u_2 \\ u_3 \end{bmatrix}, \quad u^2 = \begin{bmatrix} u_4 \\ u_5 \\ u_6 \end{bmatrix}. \tag{5}$$

The gradient of the element final volume with respect to the nodal displacements can be written as:

$$\nabla\phi_e(u) = \alpha\frac{1}{\|\bar{v}\|}\begin{bmatrix} -\bar{v} \\ +\bar{v} \end{bmatrix}. \tag{6}$$

## 3. Triangle Element Definition

Figure 2 shows the geometry of the triangle element for a 3D space. The nodes are labeled 1, 2 and 3 while traversing the sides in counterclockwise fashion. Each side is labeled with the number of its opposite node. The nodal displacements transform the element from its initial state to its final state.

$$\bar{v}^1 = v^1 + u^3 - u^2 \tag{7}$$

$$\bar{v}^2 = v^2 + u^1 - u^3 \tag{8}$$

$$\bar{v}^3 = v^3 + u^2 - u^1 \tag{9}$$

$$w = v^1 \times v^2 \tag{10}$$

$$\bar{w} = \bar{v}^1 \times \bar{v}^2. \tag{11}$$

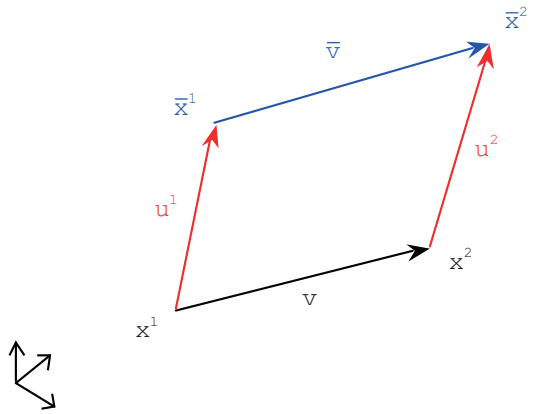


Fig. 1.

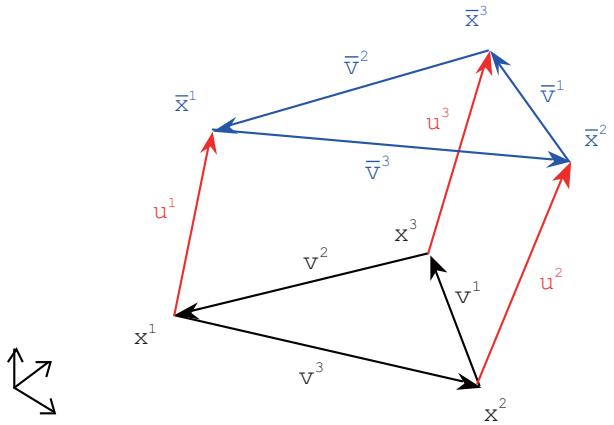


Fig. 2.

The previous expression can be written as:

$$\begin{aligned}\bar{w} &= w \\ &+v^1 \times u^1 + v^2 \times u^2 + v^3 \times u^3 \\ &+u^1 \times u^2 + u^2 \times u^3 + u^3 \times u^1. \end{aligned} \tag{12}$$

The vectors $w$ and $\bar{w}$ are orthogonal to the element in the initial state and final state respectively. Note that these vectors point toward the observer.

### 3.1 Element final volume

Supposing that the triangle element has a fixed thickness $\lambda$, its final volume can be written as:

$$\phi_e(u) = \frac{\lambda}{2}\|\bar{w}\|. \tag{13}$$

### 3.2 Gradient of the element final volume

The derivatives of the element final volume with respect to the nodal displacements can be written as:

$$\frac{d\phi_e}{du_i^j} = \frac{\lambda}{2\|\bar{w}\|}\left(\bar{w}_1\frac{\partial \bar{w}_1}{\partial u_i^j} + \bar{w}_2\frac{\partial \bar{w}_2}{\partial u_i^j} + \bar{w}_3\frac{\partial \bar{w}_3}{\partial u_i^j}\right). \tag{14}$$

The nodal displacements vectors are numbered according to its node numbers. Their individual components are numbered as follows:

$$u^1 = \begin{bmatrix} u_1 \\ u_2 \\ u_3 \end{bmatrix}, \quad u^2 = \begin{bmatrix} u_4 \\ u_5 \\ u_6 \end{bmatrix}, \quad u^3 = \begin{bmatrix} u_7 \\ u_8 \\ u_9 \end{bmatrix}. \tag{15}$$

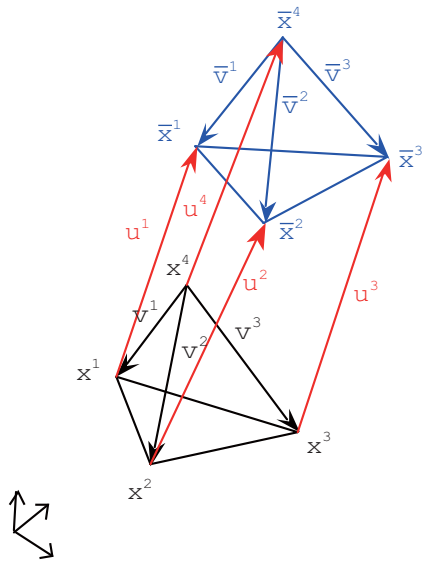


Fig. 3.

The gradient of the element final volume can be written as:

$$\nabla\phi_e(u) = \frac{\lambda}{2\|\bar{w}\|}\begin{bmatrix} \bar{w}\times\bar{v}^1 \\ \bar{w}\times\bar{v}^2 \\ -\bar{w}\times\bar{v}^1 - \bar{w}\times\bar{v}^2 \end{bmatrix}. \tag{16}$$

## 4. Tetrahedron Element Definition

Figure 3 shows the geometry of the tetrahedron element. The base nodes are labeled 1, 2 and 3 while traversing the sides in counterclockwise fashion looking from the apex, which is labeled 4. The nodal displacements transform the element from its initial state to its final state.

$$\bar{v}^1 = v^1 + u^1 - u^4 \tag{17}$$
$$\bar{v}^2 = v^2 + u^2 - u^4 \tag{18}$$
$$\bar{v}^3 = v^3 + u^3 - u^4. \tag{19}$$

### 4.1 Element final volume

The final volume of the tetrahedron element can be written as:

$$\phi_e(u) = -\frac{1}{6}(\bar{v}^1)^T(\bar{v}^2 \times \bar{v}^3). \tag{20}$$

Note that if the apex moves below the base, the volume becomes negative.

$$\left.\begin{aligned}\bar{v}^1 &= v^1 + u^1 - u^4 \\ \bar{v}^2 &= v^2 + u^2 - u^4 \\ \bar{v}^3 &= v^3 + u^3 - u^4\end{aligned}\right\} \Rightarrow \tag{21}$$

$$\begin{aligned}&\phi_e(u) \\ &= -\frac{1}{6}(v^1 + u^1 - u^4)^T\left[(v^2 + u^2 - u^4) \times (v^3 + u^3 - u^4)\right]\end{aligned} \tag{22}$$

$$d^i = u^i - u^4 \Rightarrow \tag{23}$$

$$\begin{aligned}&-6\phi_e(u) = (v^1)^T(v^2 \times v^3) \\ &+(d^1)^T(v^2 \times v^3) + (d^2)^T(v^3 \times v^1) + (d^3)^T(v^1 \times v^2) \\ &+(v^1)^T(d^2 \times d^3) + (v^2)^T(d^3 \times d^1) + (v^3)^T(d^1 \times d^2) \\ &+(d^1)^T(d^2 \times d^3).\end{aligned} \tag{24}$$

### 4.2 Gradient of the element final volume

The nodal displacements vectors are numbered according to its node numbers. Their individual components are numbered as follows:

$$u^1 = \begin{bmatrix} u_1 \\ u_2 \\ u_3 \end{bmatrix}, u^2 = \begin{bmatrix} u_4 \\ u_5 \\ u_6 \end{bmatrix}, u^3 = \begin{bmatrix} u_7 \\ u_8 \\ u_9 \end{bmatrix}, u^4 = \begin{bmatrix} u_{10} \\ u_{11} \\ u_{12} \end{bmatrix}. \tag{25}$$

The gradient of the element final volume can be written as:

$$\nabla\phi_e(u) = \frac{1}{6}\begin{bmatrix} \bar{v}^3 \times \bar{v}^2 \\ \bar{v}^1 \times \bar{v}^3 \\ \bar{v}^2 \times \bar{v}^1 \\ -\bar{v}^3 \times \bar{v}^2 - \bar{v}^1 \times \bar{v}^3 - \bar{v}^2 \times \bar{v}^1 \end{bmatrix}. \tag{26}$$

## 5. Isovolumetric Element Definition

An element that does not change its volume is desirable for many problems types. Ideally, the volume change should be zero for the isovolumetric element in its final state.

### 5.1 Constraint function

Considering $\phi_e^0$ as the initial volume, a constraint function associated with the element can be defined as:

$$\varphi_e(u) = \frac{\phi_e(u) - \phi_e^0}{\phi_e^0}. \tag{27}$$

An element with constant volume satisfies the following equation:

$$\varphi_e(u) = 0. \tag{28}$$

A tolerance for the constraint violation implies that the relative volume change is less than or equal this tolerance. Note that the element can change its shape while keeping a constant volume.

### 5.2 Gradient of the constraint function

The gradient of the constraint function with respect to the nodal displacements of the element can be written as:

$$\nabla\varphi_e(u) = \frac{1}{\phi_e^0}\nabla\phi_e(u). \tag{29}$$

#### 5.2.1 Line element

$$\nabla\varphi_e(u) = \frac{1}{\|v\|\|\bar{v}\|}\begin{bmatrix} -\bar{v} \\ +\bar{v} \end{bmatrix}. \tag{30}$$

#### 5.2.2 Triangle element

$$\nabla\varphi_e(u) = \frac{1}{\|w\|\|\bar{w}\|}\begin{bmatrix} \bar{w} \times \bar{v}^1 \\ \bar{w} \times \bar{v}^2 \\ -\bar{w} \times \bar{v}^1 - \bar{w} \times \bar{v}^2 \end{bmatrix}. \tag{31}$$

#### 5.2.3 Tetrahedron element

$$\nabla\varphi_e(u) = \frac{1}{(v^1)^T(v^3 \times v^2)} \cdot \begin{bmatrix} \bar{v}^3 \times \bar{v}^2 \\ \bar{v}^1 \times \bar{v}^3 \\ \bar{v}^2 \times \bar{v}^1 \\ -\bar{v}^3 \times \bar{v}^2 - \bar{v}^1 \times \bar{v}^3 - \bar{v}^2 \times \bar{v}^1 \end{bmatrix}. \tag{32}$$

### 5.3 Severe cancellation

Inaccuracy often results from severe cancellation that occurs when nearly equal values are subtracted (Goldberg, 1991). Note that inaccuracy can result from the difference between the final and initial volumes because they can be arbitrarily close for the isovolumetric element. However, severe cancellation can usually be eliminated by algebraic reformulation. The constraint function associated with the element, reformulated to avoid severe cancellation, can be written for the line, triangle and tetrahedron elements.

#### 5.3.1 Line element

$$\|v\|\hat{v} = v \tag{33}$$

$$\|v\|z = u^2 - u^1 \tag{34}$$

$$\varphi_e(u) = \frac{z^T(2\hat{v} + z)}{\|\hat{v} + z\| + 1}. \tag{35}$$

#### 5.3.2 Triangle element

$$\|w\|\hat{w} = w \tag{36}$$

$$\begin{aligned} \|w\|z = {} & (v^1 - u^2) \times u^1 \\ & + (v^2 - u^3) \times u^2 \\ & + u^3 \times (v^1 + v^2 + u^1) \end{aligned} \tag{37}$$

$$\varphi_e(u) = \frac{z^T(2\hat{w} + z)}{\|\hat{w} + z\| + 1}. \tag{38}$$

#### 5.3.3 Tetrahedron element

$$\|v^i\|\hat{v}^i = v^i \tag{39}$$

$$\|v^i\|z^i = u^i - u^4 \tag{40}$$

$$\begin{aligned} (\hat{v}^1)^T(\hat{v}^2 \times \hat{v}^3)\varphi_e(u) = {} & (\hat{v}^1)^T(\hat{v}^2 + z^2) \times z^3 \\ & + (\hat{v}^2)^T(\hat{v}^3 + z^3) \times z^1 \\ & + (\hat{v}^3)^T(\hat{v}^1 + z^1) \times z^2 \\ & + (z^1)^T(z^2) \times z^3). \end{aligned} \tag{41}$$

## 6. The Geometrical Minimal Shape Problem

The geometrical minimal shape problem can be written as an equality constrained minimization problem, with one constraint for each isovolumetric element, as:

$$\min \pi(u) = \sum_e \phi_e(u) \tag{42}$$

$$\text{subject to } \varphi_e(u) = 0. \tag{43}$$

### 6.1 Augmented lagrangian method

Historically, the quadratic penalty method was the first method used for constrained nonlinear programming. Due to its simplicity, it is still used in practice, although it has an important computational disadvantage. The augmented Lagrangian method is related to the quadratic penalty method, but it reduces the possibility of ill conditioning by introducing Lagrange multiplier estimates into the function to be minimized. Consider $\mu$ as the penalty parameter, $y$ as the vector of Lagrange multipliers and that the subscript $e$ stands for a particular element. The augmented Lagrangian function and its gradient can be written as:

$$\pi(u, y, \mu) = \sum_e \phi_e(u) + \sum_e \left[\frac{\mu}{2}\varphi_e(u) - y_e\right]\varphi_e(u) \tag{44}$$

$$\nabla_u\pi(u, y, \mu) = \sum_e \nabla\phi_e(u) + \sum_e \left[\mu\varphi_e(u) - y_e\right]\nabla\varphi_e(u). \tag{45}$$

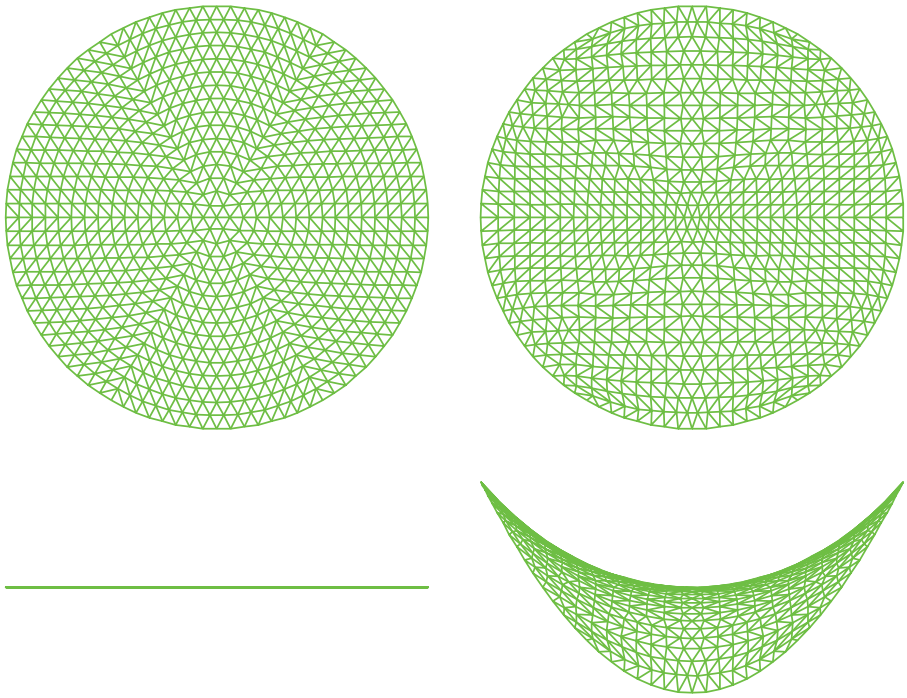

Fig. 4.

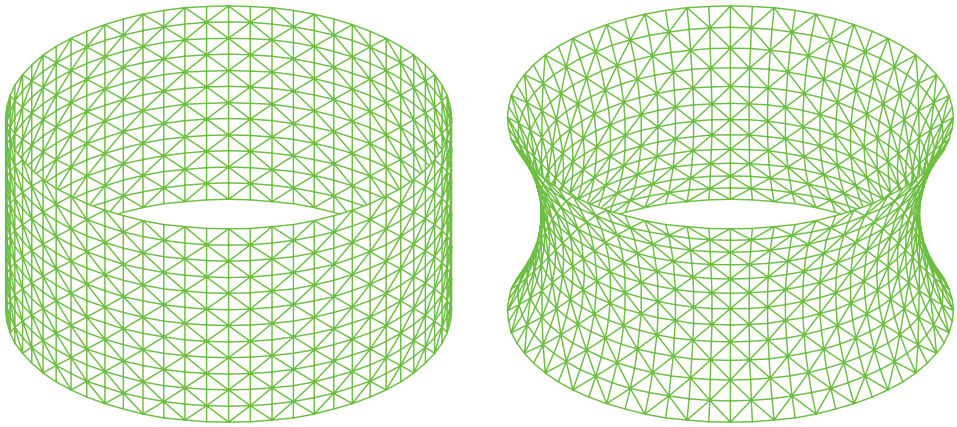

Fig. 5.

The following algorithm was adapted from Conn *et al.* (2010). The scalar $\mu$ is the penalty parameter. The vector $y$ is the vector of Lagrange multipliers. The tolerance $\omega$ is used to find an approximate solution with the current value of the penalty parameter and the current estimates of the Lagrange multipliers. The tolerance $\eta$ is used to check if the current value of the penalty parameter is producing an acceptable level of relative volume change of the isovolumetric elements. As the iterations proceed, the Lagrange multipliers are updated, the penalty parameter is increased and the tolerances are tightened. The iterations terminate if the infinity norm of the gradient of the augmented Lagrangian function becomes less than or equal to $\omega_*$ and the maximum relative volume change of the isovolumetric elements becomes less than or equal to $\eta_*$.

Choose $u$, $y$, $\mu$, $\eta_*$ and $\omega_*$;

$$\eta \leftarrow \frac{1}{\mu^{0.1}};$$

$$\omega \leftarrow \frac{1}{\mu};$$

**while** $\max |\varphi_e(u)| > \eta_*$ or $\|\nabla_u \pi(u, y, \mu)\|_\infty > \omega_*$
**loop**
  Minimize $\pi(u, y, \mu)$ until $\|\nabla_u \pi(u, y, \mu)\|_\infty \leq \omega$;
  **if** $\max |\varphi_e(u)| \leq \eta$
    $y_e \leftarrow y_e - \mu \varphi_e(u)$;
    $\eta \leftarrow \frac{\eta}{\mu^{0.9}}$;
    $\omega \leftarrow \frac{\omega}{\mu}$;
  **else**
    $\mu \leftarrow 10\mu$;
    $\eta \leftarrow \frac{1}{\mu^{0.1}}$;
    $\omega \leftarrow \frac{1}{\mu}$;
  **end if**;
**end loop**;

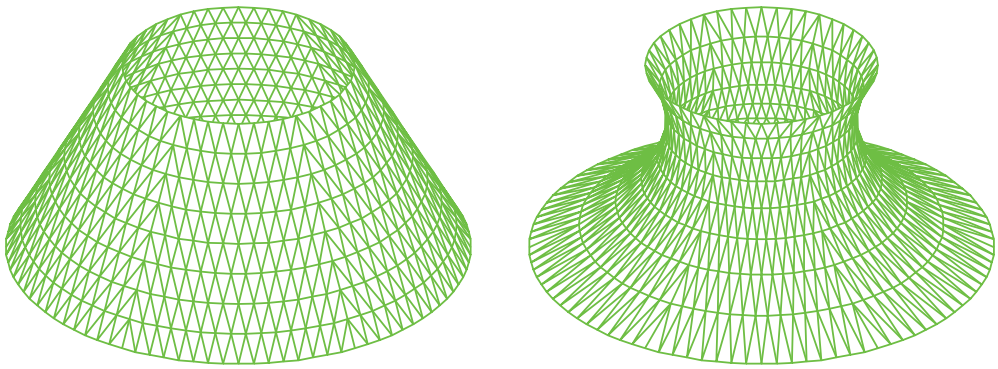

Fig. 6.

Table 1.

| Elements | $y(0)$ | Error (%) |
|---|---|---|
| 384 | 0.8470554 | 0.15 |
| 1536 | 0.8480256 | 0.04 |
| 6144 | 0.8482543 | 0.01 |

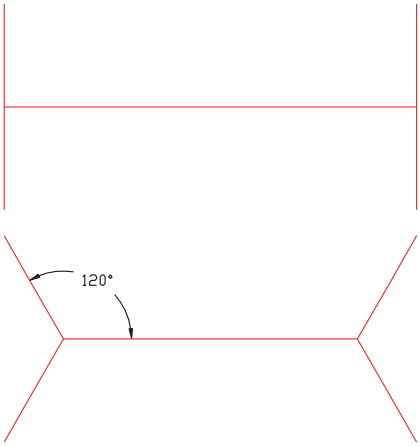


Fig. 7.

It is interesting to note that one special type of geometrical minimal shape problem, composed only of line elements, can be used to define the form of tensegrity structures. A review of the important literature related to form finding methods for tensegrity structures is given by Tibert and Pellegrino (2003) and more recently by Juan and Tur (2008).

## 7. Nonlinear Programming Problem

In order to find the local minimum points of a nonlinear multivariate function, the general strategy that can be used is: Choose a starting point and move in a given direction such that the function decreases. Find the minimum point in this direction and use it as a new starting point. Continue this way until a local minimum point is reached. The problem of finding the minimum points of a nonlinear multivariate function is replaced by a sequence of sub problems, each one consisting of finding the minimum of a univariate nonlinear function. In quasi-Newton methods, starting with the unit matrix, a positive definite approximation to the inverse of the Hessian matrix is updated at each iteration. This update is made using only values of the gradient vector. A direction such that the function decreases is calculated as minus the product of this approximation of the inverse of the Hessian matrix and the gradient vector calculated at the starting point of each iteration. Consequently, it is not necessary to solve any system of equations. Moreover, the analytical derivation of an expression for the Hessian matrix is not necessary. Note that by minimizing a function it is almost impossible to find a local maximum point. The only exception is that it is possible to find a saddle point, that is, the point is a local minimum and also a local maximum. However, even in this improbable situation, a direction of negative curvature to continue toward a local minimum point can be found as described by Gill and Murray (1974). The computer code uses the limited memory BFGS to tackle large scale problems as described by Nocedal and Wright (2006). It also employs a line search procedure through cubic interpolation as described by Nocedal and Wright (2006).

## 8. Examples

The primary colors red, green and blue are used for the line, triangle and tetrahedron elements respectively. The secondary colors cyan, magenta and yellow are used for the isovolumetric line, triangle and tetrahedron elements respectively. The usual parameters used in the examples are $\mu_0 = 10^3$, $\omega^* = 10^{-3}$ and $\eta^* = 10^{-5}$.

**Example 1:** An initially flat circular surface with thickness $= 2$, radius $r = 1$ and the boundary displaced according to the following hyperbolic paraboloid equation, where $h = 1/2$. Figure 4 shows the meshes for the initial and final surfaces.

$$z = h\left[\left(\frac{x}{r}\right)^2 - \left(\frac{y}{r}\right)^2\right].$$

**Example 2:** A cylinder with thickness $= 1$, radius $r = 1$ and height $h = 1$. Figure 5 shows the meshes for the initial and final surfaces.

The final surface is symmetrical about the $Z$ axis. The following analytical solution for the cross-section of the surface in the $YZ$ plane is described by Isenberg (1992).

$$y(z) = c\cos h\left(\frac{z}{c}\right).$$

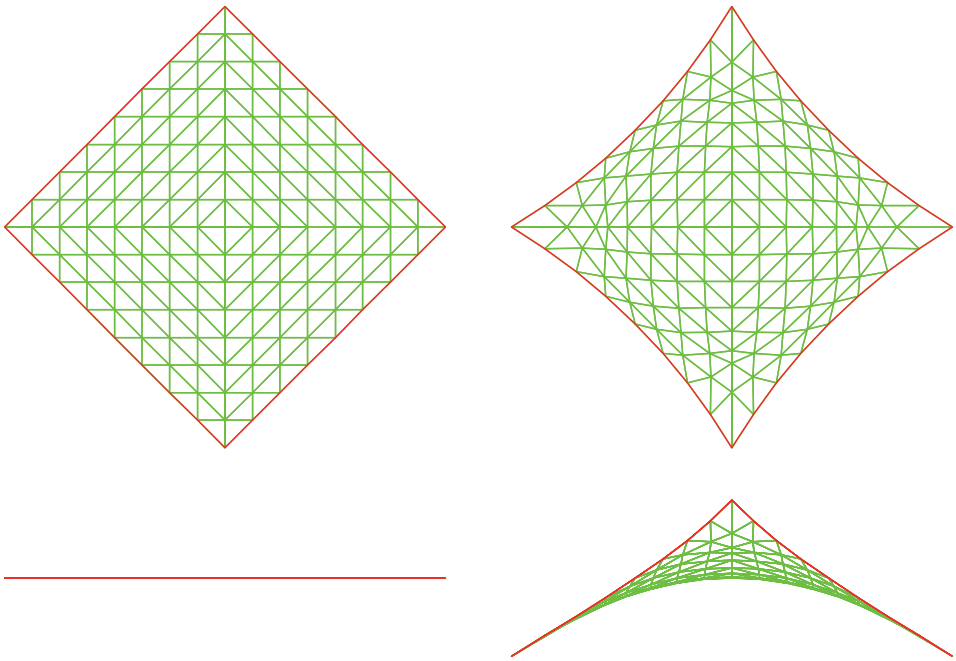

Fig. 8.

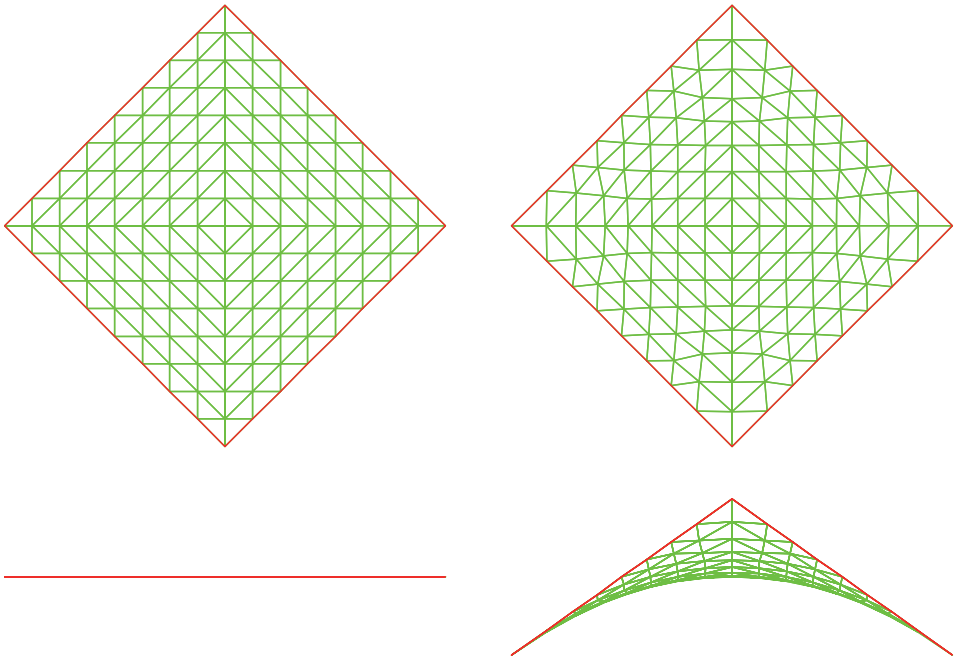

Fig. 9.

Note that $y(0) = c$. The value $c$ is a solution of the following equation. In this example, $c = 0.8483379$.

$$\frac{2r}{h} = \frac{2c}{r}\cos h\left(\frac{h}{2c}\right).$$

Table 1 shows the relative error for $y(0)$ with different initial meshes.

**Example 3:** A frustum cone with thickness = 2, upper radius = 0.5, lower radius = 1 and height = 0.9. Figure 6 shows the meshes for the initial and final surfaces.

**Example 4:** On the top, Fig. 7 shows an initial path through the corner points of a rectangle with horizontal dimension equal to 4 and vertical dimension equal to 2. The line elements have area = 1. On the bottom, Fig. 7 shows the final path.

The general problem of connecting n points by the shortest path length is called Steiner problem (Isenberg, 1992). Its solution contains straight lines intersecting at 120°. The number of intersections is between zero and $(n-2)$.

**Example 5:** An initially flat square surface with thickness = 1, side = 1 and two opposite corners displaced by $+1/2$ while the two other opposite corners displaced by $-1/2$. The edges have line elements with area = 5. Figure 8 shows

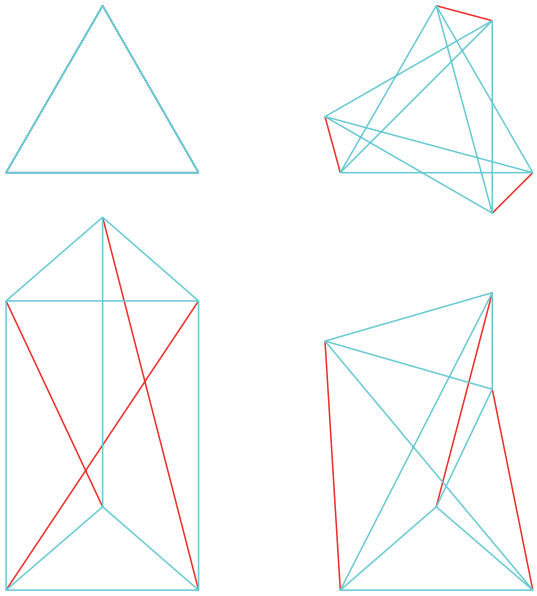

Fig. 10.

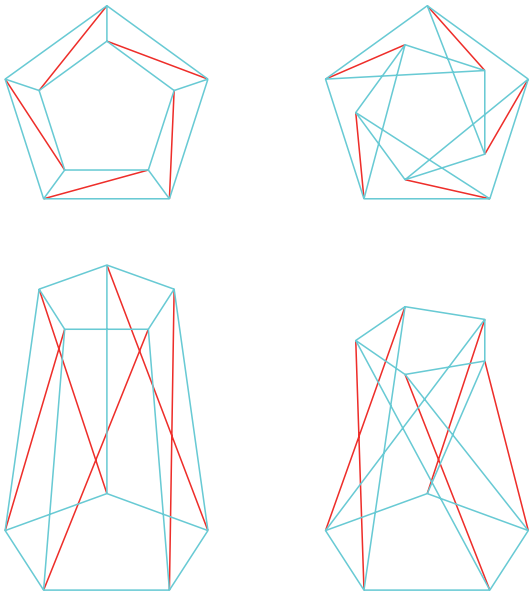

Fig. 11.

Table 2.

| Node | Coord-X | Coord-Y | Coord-Z |
|---|---|---|---|
| 1 | $-s/2$ | $-r/2$ | $h$ |
| 2 | $s/2$ | $-r/2$ | $h$ |
| 3 | 0 | $r$ | $h$ |
| 4 | 0 | $-2r$ | $h$ |
| 5 | $s$ | $r$ | $h$ |
| 6 | $-s$ | $r$ | $h$ |
| 7 | $s$ | $-r$ | $-h$ |
| 8 | $-s$ | $-r$ | $-h$ |
| 9 | 0 | $2r$ | $-h$ |
| 10 | 0 | $-r$ | $-h$ |
| 11 | $-s/2$ | $r/2$ | $-h$ |
| 12 | $s/2$ | $r/2$ | $-h$ |

Table 3.

| Elem | Node | Node |
|---|---|---|
| 3 | 4 | 11 |
| 6 | 5 | 10 |
| 9 | 6 | 12 |
| 12 | 7 | 1 |
| 15 | 8 | 3 |
| 18 | 9 | 2 |

the meshes for the initial and final surfaces.

Note that minimizing the total volume results in opposite effects on the lengths of the free edges. It tends to decrease the surface area defined by the triangle elements and consequently tends to increase the lengths of the free edges. It tends to decrease the path lengths defined by the line elements and consequently tends to decrease the lengths of the free edges. In this example, the free edges are curved due to relatively small value for the areas of the line elements.

Table 4.

| Elem | Area | Length |
|---|---|---|
| 3 | $-1.25$ | 1.4563 |
| 6 | $-1.50$ | 1.5654 |
| 9 | $-1.75$ | 1.6297 |
| 12 | $-2.00$ | 1.8555 |
| 15 | $-2.25$ | 1.8875 |
| 18 | $-2.50$ | 1.8884 |

Table 5.

| Elem | Area | Length |
|---|---|---|
| 3 | $-1.00$ | 1.7321 |
| 6 | $-1.00$ | 1.7321 |
| 9 | $-1.00$ | 1.7321 |
| 12 | $-1.00$ | 1.7320 |
| 15 | $-1.00$ | 1.7321 |
| 18 | $-1.00$ | 1.7320 |

**Example 6:** An initially flat square surface with thickness $= 1$, side $= 1$ and two opposite corners displaced by $+1/2$ while the two other opposite corners displaced by $-1/2$. The edges have line elements with area $= 500$. Figure 9 shows the meshes for the initial and final surfaces.

Note that minimizing the total volume results in opposite effects on the lengths of the free edges. It tends to decrease the surface area defined by the triangle elements and consequently tends to increase the lengths of the free edges. It tends to decrease the path lengths defined by the line elements and consequently tends to decrease the lengths of the free edges. In this example, the free edges are straight due to relatively big value for the areas of the line elements.

**Example 7:** A straight prismoid with height $= 3$. The bottom and top regular triangles are inscribed in a circle of

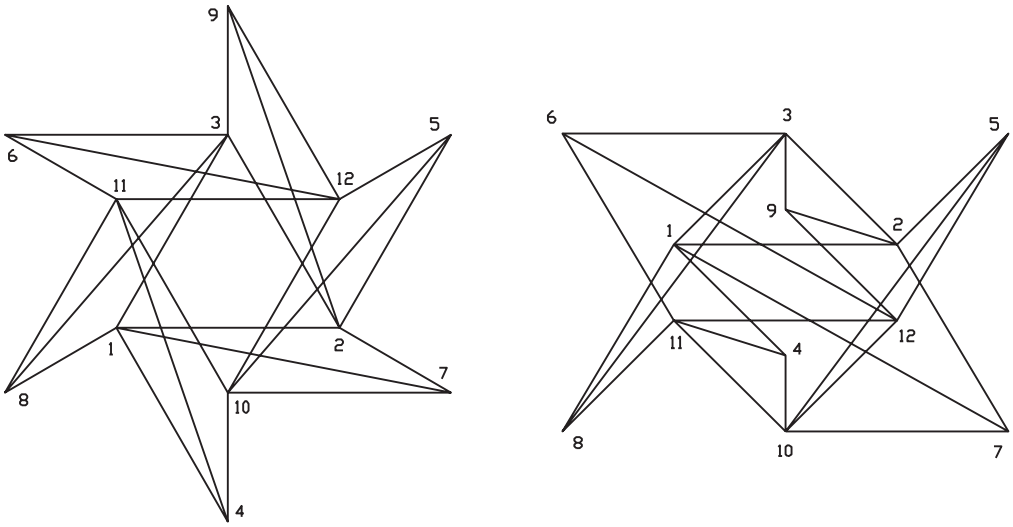


Fig. 12.

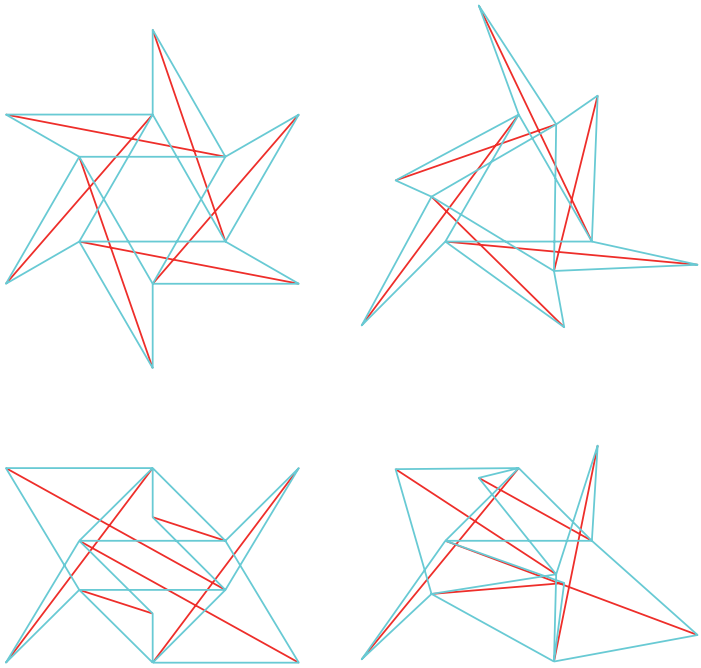

Fig. 13.

radius = 1. It is composed by 3 line elements and 9 isovolumetric line elements. The line elements have area = 1. The penalty parameter = 1.0E+03. The top triangle rotates 150 degrees clockwise relatively to the bottom triangle. Figure 10 shows the initial and final shapes.

**Example 8:** A straight prismoid with height = 2. The bottom and top regular pentagons are inscribed in a circle of radius = 0.75 and 0.5 respectively. It is composed by 5 line elements and 15 isovolumetric line elements. The line elements have area = 1. The penalty parameter = 1.0E+03. The top pentagon rotates 126 degrees clockwise relatively to the bottom pentagon. Figure 11 shows the initial and final shapes.

**Example 9:** Figure 12 shows the geometry of a sculpture called Stella Octangula, which was proposed by David Georges Emmerich. He was a Hungarian architect, sculptor and author. An extensive description of his works is given by Chassagnoux (2006). An analysis of this tensegrity structure is described by Motro (2011).

The geometry is composed by 18 elements with length equal to $s$ and 6 diagonal elements with length equal to $s\sqrt{3}$. Table 2 shows the coordinates of the vertices, where the parameters $r$ and $h$ are given by:

$$r = \frac{s}{\sqrt{3}}$$
$$h = \frac{s}{\sqrt{6}}.$$

Table 3 shows the connectivity of the diagonal elements.

A Stella Octangula with parameter $s = 1$ and support constraints on nodes 1, 2 and 3 to prevent rigid body mo-

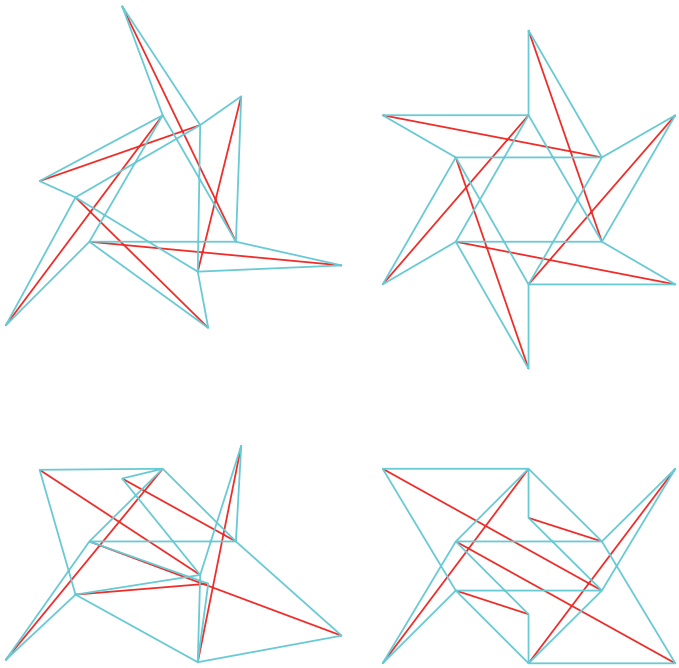

Fig. 14.

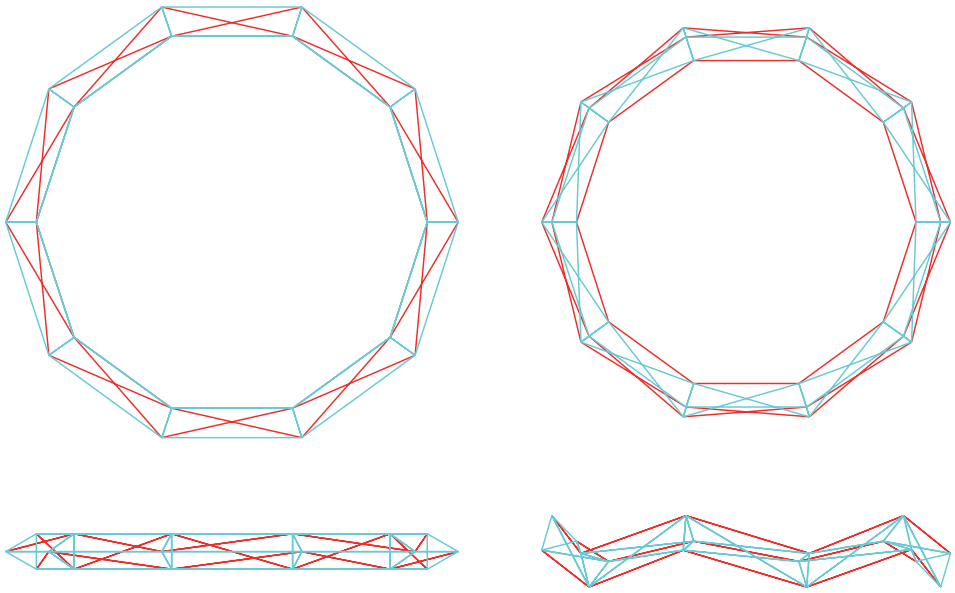

Fig. 15.

tion. A nonregular Stella Octangula is generated by imposing different areas for selected elements of a regular Stella Octangula. Excluding the diagonal elements, all other elements are isovolumetric elements with area = 1. The areas for the diagonal elements in the initial shape and the lengths of the diagonal elements in the final shape are shown in Table 4.

Figure 13 shows the initial shape (regular Stella Octangula) on the left and the final shape (nonregular Stella Octangula) on the right.

**Example 10:** The regular Stella Octangula is recovered by imposing equal areas for the same selected elements on the previously generated nonregular Stella Octangula. The areas for the diagonal elements in the initial shape and the lengths of the diagonal elements in the final shape are shown in Table 5.

Figure 14 shows the initial shape (nonregular Stella Octangula) on the left and the final shape (regular Stella Octangula) on the right.

**Example 11:** A circular prismoid with axis on a circumference of radius = 10. The section is defined by a regular triangle inscribed in a circle of radius = 1. It is composed by 30 line elements and 60 isovolumetric line elements. The line elements have area = 1. The penalty parameter = 1.0E+03. Figure 15 shows the initial and final shapes.

**Example 12:** A square with side = 1 composed by 8 isovol-

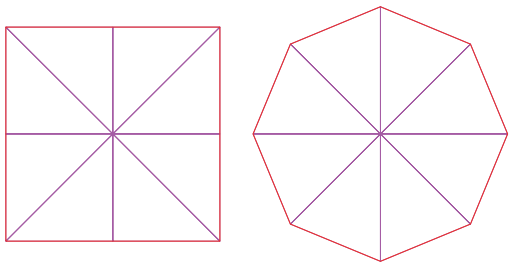

Fig. 16.

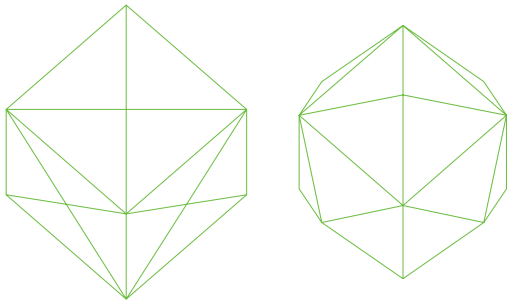

Fig. 17.

umetric triangle elements with thickness = 10. The square's perimeter has line elements with area = 1. The penalty parameter = 1.0E+03. The triangle elements preserve the square's area while the line elements minimize its perimeter. The square turns into an octagon. Figure 16 shows the initial and final areas.

**Example 13:** A cube with side = 2 composed by 24 isovolumetric tetrahedron elements. The cube's surface has triangle elements with thickness = 1. The penalty parameter = 1.0E+03. The tetrahedron elements preserve the cube's volume while the triangle elements minimize its surface. The cube turns into a 24 faces polyhedron. Figure 17 shows the initial and final volumes.

## 9. Conclusion

This text describes a novel mathematical model that unifies all geometrical minimal shape problems by defining geometrical finite elements. Three types of elements are defined: line, triangle and tetrahedron. By associating a volume for each element type, the line, triangle and tetrahedron elements can be used together in the discretization of a geometrical shape. For each element type, its corresponding isovolumetric element is also defined. The geometrical minimal shape problem is formulated as an equality constrained minimization problem. The importance of this approach is that apparently distinct problems can be treated by a unified framework.

A special application is the form finding of structures: tensile fabric structure with constrained edges as shown by example 1, hyperboloid cooling tower as shown by example 3, tensile fabric structure with free edges as shown by examples 5 and 6, tensegrity structure as shown by examples 7, 8, 9, 10 and 11. Example 4 is a classical Steiner problem. Examples 12 and 13 are simple geometrical problems whose solution can be intuitively imagined. They were included to show the correctness of the mathematical model.

## References

Chassagnoux, A. (2006) David Georges Emmerich Professor of morphology, *International Journal of Space Structures*, **21**, 59–71.

Conn, A. R., Gould, G. I. M., Toint, P. L. (2010) *Lancelot: A Fortran Package for Large-Scale Nonlinear Optimization*, Springer-Verlag, Berlin Heidelberg.

Gill, P. E. and Murray, W. (1974) Newton type methods for unconstrained and linearly constrained optimization, *Mathematical Programming*, **7**, 311–350.

Goldberg, D. (1991) What every computer scientist should know about floating-point arithmetic, *ACM Computing Surveys*, **23**, 5–48.

Isenberg, C. (1992) *The Science of Soap Films and Soap Bubbles*, Dover Publications, New York.

Juan, S. H. and Tur, J. M. M. (2008) Tensegrity frameworks: Static analysis review, *Mechanism and Machine Theory*, **43**, 859–881.

Motro, R. (2011) Structural morphology of tensegrity systems, *Meccanica*, **46**, 27–40.

Nocedal, J. and Wright, S. J. (2006) *Numerical Optimization*, 2nd ed., Springer Science, New York.

Tibert, A. G. and Pellegrino, S. (2003) Review of form-finding methods for tensegrity structures, *International Journal of Space Structures*, **18**, 209–223.